

Sodium-cooled fast reactor (SFR) fuel assembly design with graphite-moderating rods to reduce the sodium void reactivity coefficient



Jong Hyuck Won, Nam Zin Cho*, Hae Min Park, Yong Hoon Jeong**

Department of Nuclear and Quantum Engineering, Korea Advanced Institute of Science and Technology, 291 Daehak-ro, Yuseong-gu, Daejeon 305-701, Republic of Korea

HIGHLIGHTS

- The graphite rod-inserted SFR fuel assembly is proposed to achieve low sodium void reactivity.
- The neutronics/thermal-hydraulics analyses are performed for the proposed SFR cores.
- The sodium void reactivity is improved about 960–1030 pcm compared to reference design.

ARTICLE INFO

Article history:

Received 10 December 2013

Received in revised form 13 October 2014

Accepted 17 October 2014

ABSTRACT

The concept of a graphite-moderating rod-inserted sodium-cooled fast reactor (SFR) fuel assembly is proposed in this study to achieve a low sodium void reactivity coefficient. Using this concept, two types of SFR cores are analyzed; the proposed SFR type 1 core has new SFR fuel assemblies at the inner/mid core regions while the proposed SFR type 2 core has a B₄C absorber sandwich in the middle of the active core region as well as new SFR fuel assemblies at the inner/mid core regions. For the proposed SFR core designs, neutronics and thermal-hydraulic analyses are performed using the DIF3D, REBUS3, and the MATRA-LMR codes.

In the neutronics analysis, the sodium void reactivity coefficient is obtained in various void situations. The two types of proposed core designs reduce the sodium void reactivity coefficient by about 960–1030 pcm compared to the reference design. However, the TRU enrichment for the proposed SFR core designs is increased. In the thermal hydraulic analysis, the temperature distributions are calculated for the two types of proposed core designs and the mass flow rate is optimized to satisfy the design constraints for the highest power generating assembly.

The results of this study indicate that the proposed SFR assembly design concept, which adopts graphite-moderating rods which are inserted into the fuel assembly, can feasibly minimize the sodium void reactivity coefficient. Single TRU enrichment and an identical fuel slug diameter throughout the SFR core are also achieved because the radial power peak can be flattened by varying the number of moderating rods in each core region.

© 2014 Elsevier B.V. All rights reserved.

1. Introduction

Currently, PWRs (pressurized water-cooled reactors) are one of the main reactor types for commercial nuclear power plants. However, uranium utilization in PWRs is low because thermal neutrons are used for the fission reaction. Therefore, the burden of PWR spent

fuel and nuclear waste will become a major problem in the nuclear industry in the not-too-distant future.

For sustainable nuclear power generation, waste minimization and effective uranium resource utilization should be achieved in next-generation nuclear power plants. There are many ongoing research activities related to next-generation nuclear reactors. Examples include the SFR (sodium-cooled fast reactor) and the VHTR (very-high-temperature gas-cooled reactor). Among these, the SFR core type may be the most viable means of solving current issues. It uses fast neutrons for the nuclear fission reaction and can therefore burn TRU (trans-uranic) isotopes for power generation.

* Corresponding author. Tel.: +82 42 350 3819; fax: +82 42 350 3810.

** Corresponding author. Tel.: +82 42 350 3826; fax: +82 42 350 3810.

E-mail addresses: nzcho@kaist.ac.kr (N.Z. Cho), jeongyh@kaist.ac.kr (Y.H. Jeong).

It can also breed plutonium from U-238. In other words, uranium can be utilized more efficiently and long-lived radioactive isotopes can be destroyed. In terms of thermal hydraulics and materials, liquid sodium is an excellent material as a coolant due to its high thermal conductivity, low density, high boiling point and good material compatibility with the fuel and structural materials.

For a SFR, the sodium void reactivity becomes positive, as the sodium coolant acts as a moderator for fast neutrons. Generally, current designs of large SFRs exhibit sodium void reactivity coefficients of 4\$–6\$. This value represents an important obstacle to licensing. For this reason, there have been many attempts by researchers to reduce the sodium void reactivity (Khalil and Hill, 1991; Chang et al., 1991; Rachi et al., 1997). These studies can be categorized into two types: those that increase the neutron leakage from the SFR core, and those that involve neutron spectrum softening. The first approach reduces the ratio of the core height to the diameter and/or introduces an absorber region at the active core to decouple the reactor into upper and lower regions. The second approach introduces a ZrH layer as a moderator (Rachi et al., 1997).

Recently, at KAERI (Korea Atomic Energy Research Institute) in Korea, a conceptual design of the KALIMER-600 core was developed. It uses single-enriched TRU fuel throughout the SFR core, while the radial power peak is flattened by means of different fuel slug diameters for each active core region (Hahn et al., 2007). Previously, a ZrH moderating rod, a B₄C absorbing rod, and a dummy fuel rod were used with the same fuel slug diameter in the KALIMER conceptual design to soften the neutron spectrum and reduce radial power peaking. However, there is an irradiation issue pertaining to hydride materials at high temperatures. Hence, the non-fuel rod concept was canceled.

KAIST (Korea Advanced Institute of Science and Technology) has also studied the concept of non-fuel rod insertion into the fuel assembly to reduce the sodium void reactivity coefficient. To avoid the irradiation problem of hydride materials, graphite is as the non-fuel rod instead of ZrH. In the SFR design proposed in this study, the radial power peak is reduced by replacing some fuel rods with graphite-moderating rods, while the same fuel slug diameter and single-enrichment are used throughout the reactor core. This graphite-moderating rod-insertion concept has two main benefits. First, it softens the neutron spectrum to reduce the sodium void reactivity with moderating rods even with a sodium void, and second, it reduces the fabrication cost through the use of single-enriched fuel and an identical fuel slug diameter. Therefore, in this paper, the effect of adopting graphite-moderating rods to reduce the sodium void reactivity is reported.

This paper consists of four parts. First, the detailed design features and configuration of the proposed SFR core are presented in Section 2. Second, the calculation methods/procedures pertaining to the neutronics and core thermal-hydraulics analyses are presented in Section 3. Third, the numerical results of both the neutronics analysis and the thermal-hydraulics performance assessments are given in Section 4. Finally, the summary and conclusions are given in Section 5.

2. Design description

2.1. Fuel assembly with moderating rods

Before introducing the SFR core design, the assembly design will be discussed, as the replacement of some fuel rods with graphite-moderating rods in a fuel assembly is a major feature of this study.

The detailed design of the fuel assembly in this study is based on the KALIMER-600 breakeven conceptual core (Hahn et al., 2007). This design uses 271 pins in an assembly with a modified HT9 wire

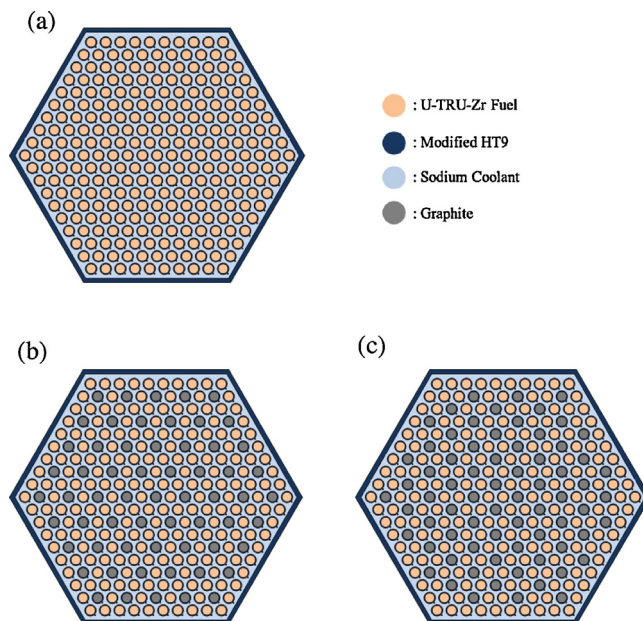


Fig. 1. SFR fuel assemblies [(a) Typical fuel assembly (271 fuel rods/0 moderating rods), (b) Moderating rod inserted fuel assembly, case 1 (210 fuel rods/61 moderating rods), and (c) Moderating rod inserted fuel assembly, case 2 (199 fuel rods/72 moderating rods).].

wrap. The fuel material is U-TRU-10%Zr metallic alloy, and modified HT9 is used as the duct and cladding material. Fig. 1 shows the three types of fuel assemblies considered in this paper.

Fig. 1(a) shows the most common type of SFR fuel assembly, which does not have any non-fuel pins. Based on this typical fuel assembly, some of the fuel rods are replaced with graphite-moderating rods. In this design, there are no absorbing rods, such as B₄C rods of the type previously used in the KALIMER design. Hence, comparatively many graphite-moderating rods are inserted into the fuel assembly to reduce the radial power peak and the sodium void reactivity coefficient.

Fig. 1(b) and (c) show two distinctly modified SFR fuel assembly configurations, one with 61 moderating rods and the other with 72.

The (Fig. 1(b)) fuel assembly denoted as case 1 has 61 graphite-moderating rods with a 1/6 periodic geometry. In this assembly, 22.51% of the fuel rods are changed to graphite rods compared to the typical SFR fuel assembly design. Case 2 (Fig. 1(c)), with 72 graphite-moderating rods (with 26.57% replaced) uses a 1/3 periodic geometry. In both of these modified fuel assemblies, fuel rods located on the side of the duct are not replaced with moderating rod due to the relatively large coolant flow area in that area.

In the modified SFR fuel assembly design, approximately 22.5–26.5% of the fuel rods are replaced with graphite rods. However, it is expected that the core thermal-hydraulics design limit can easily be met even when using this high a percentage of graphite rods for two reasons. First, the coolant flow area is identical to that used in the typical design while the number of fuel rods is reduced, and second, the thermal conductivity levels of the metallic fuel and the sodium coolant are high. A discussion is given and the numerical results of the thermal-hydraulic analysis are shown subsequently.

2.2. SFR core design description with the modified fuel assembly

The core design with the modified (graphite rod inserted) fuel assembly also increases the proliferation resistance through its use of single-enrichment fuel without a blanket. The core is designed to provide output of 1500 MWth with 365 effective full power days (EFPDs). In addition, the peak discharge fast neutron fluence is kept

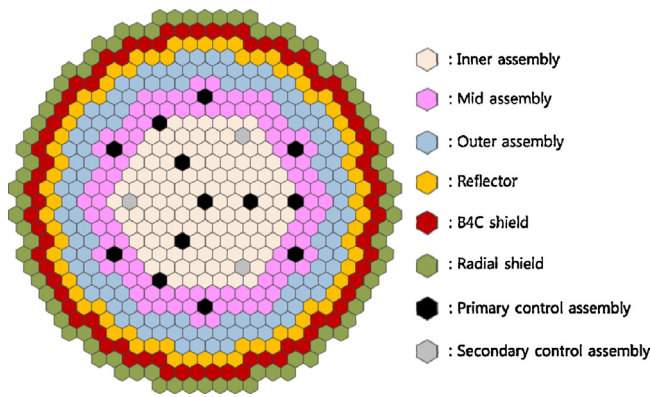


Fig. 2. Radial configuration of the SFR cores analyzed in this study.

below 4.0×10^{23} neutrons/cm³ to ensure the integrity of the material. The fuel used is U-TRU-10%Zr alloy. Its smeared density is assumed to be 75% of its theoretical density.

In this paper, three different SFR cores are analyzed. Two of them are newly proposed reactors (proposed SFR core types 1 and 2) that use the modified fuel assembly concept to achieve low sodium void reactivity, and the third one is a typical SFR core that does not use the new fuel assembly concept. It serves as a reference core for comparison.

Figs. 2 and 3 and Table 1 depict the SFR core configurations and design parameters analyzed in this study.

As shown in Fig. 2, all three SFR cores have the same radial configuration. The only difference between the proposed SFR core and the typical SFR core is that a different type of fuel assembly is used for the inner and mid-core regions. In Table 1, detailed descriptions of the fuel assemblies for each core region are shown.

For the proposed SFR cores, each active core region has a different number of fuel pins, while the other parameters, in this case the pin diameter and the cladding thickness, are identical throughout the fuel assemblies. As the number of fuel pins is decreased from the outer core region to the inner region, power flattening is achieved without fuel enrichment splitting. This is also good for the sodium void reactivity because the void effect of the inner core region is more severe than that of the outer region.

The typical SFR core is designed based on the KALIMER-600 breakeven core, which uses the same enrichment fuel but a different fuel slug diameter for each active core region. The cladding thickness of each core region is described in Table 1.

Table 1
Core design parameters in this study.

Parameter	Value		
Assembly pitch (cm)	18.713		
Duct thickness (mm)	3.7		
Duct material	Modified HT9		
Pin diameter (mm)	9.0		
Cladding material	Modified HT9		
Wire wrap diameter (mm)	1.4		
	Inner	Mid	Outer
Proposed SFR type 1/2 cores			
Cladding thickness (mm)	0.59	0.59	0.59
Number of fuel pins	199	210	271
Number of graphite pins	72	61	0
Fuel assembly configuration	Fig. 1(c)	Fig. 1(b)	Fig. 1(a)
Typical SFR core (reference core)			
Cladding thickness (mm)	1.02	0.72	0.59
Number of fuel pins	271	271	271
Number of graphite pins	0	0	0
Fuel assembly configuration	Fig. 1(a)	Fig. 1(a)	Fig. 1(a)

For the axial core configuration, two design types are considered in this study. The first is the normal design, as shown in Fig. 3(a). It consists of the bottom shielding material, the fuel region, and the upper gas plenum. The second is the design with the B₄C absorber bed with a thickness of 10 cm at the axial center of the active core region. The axial configuration of this second type is shown in Fig. 3(b). The proposed SFR type 1 core and the typical SFR core have the configuration shown in Fig. 3(a), while the proposed SFR type 2 core is shown in Fig. 3(b) for configuration.

The type 1 design reduces the sodium void reactivity due to spectrum softening stemming from the use of graphite-moderating rods in the fuel assembly. For the type 2 design, in addition to the moderating rod features, a B₄C absorber bed decouples the active core into upper and lower cores. This increases the effective neutron leakage.

3. Analysis method

3.1. Neutronics analysis

For the neutronics analysis, the KAFAX library developed by KAERI is used as the master cross-section library. It is based on the ENDF/B-VII library and has a 150-group energy structure. The KAFAX library is generated using the NJOY code (MacFarlane and Muir, 1994) with the neutron spectrum of the KALIMER core as a weighting function.

Normally, for a fast reactor analysis, a lattice calculation is not a proper approach to generate condensed and homogenized cross-sections. The isolated assembly assumption is not valid due to the long neutron mean-free path in a fast reactor core. Therefore, a fast reactor assembly is strongly coupled with neighboring assemblies. As a result, a different approach is used for fast reactor neutronics analysis. Fig. 4 shows the flow chart of the neutronics analysis of an SFR core.

Initially, the TRANSX code (MacFarlane, 1992) generates the energy self-shielded 150-group cross-section table. During this process, each SFR assembly is considered as a homogeneous mixture and the assembly-level geometric self-shielding effect is neglected. The neutron flux does not fluctuate much within the assembly in a fast reactor system; therefore, this assumption is feasible. With energy self-shielded 150-group cross sections, the simplified R-Z geometry of an SFR core is solved by a deterministic transport code. With this calculation, the neutron spectrum for each region is obtained. This is used for group condensation. This simplified reactor core analysis is required because each assembly is strongly coupled with neighboring assemblies in a fast reactor system. In this study, the TWODANT code (Alcouffe et al., 1995) is used for this step.

From this calculation flow, a group-condensed and assembly homogenized cross-section table is generated. In this study, a condensed energy structure of 25 groups is used. For the SFR core analysis, the REBUS3 code (Toppel, 1990) is used to find the equilibrium core configuration. In the REBUS3 fuel cycle calculation, the recovery factor for each isotope during the reprocessing step is assumed to be 100% for uranium isotopes, 99.9% for TRU isotopes, and 5% for rare-earth isotopes.

Finally, the DIF3D code (Derstine, 1984) steady-state calculation is used to obtain the sodium void reactivity coefficient by analyzing the sodium-filled and the sodium-voided SFR cores.

3.2. Thermal-hydraulic analysis

While core thermal-hydraulic designs of PWRs have design constraints related to the critical heat flux due to the low boiling temperature of the water coolant and the phase changes, the core

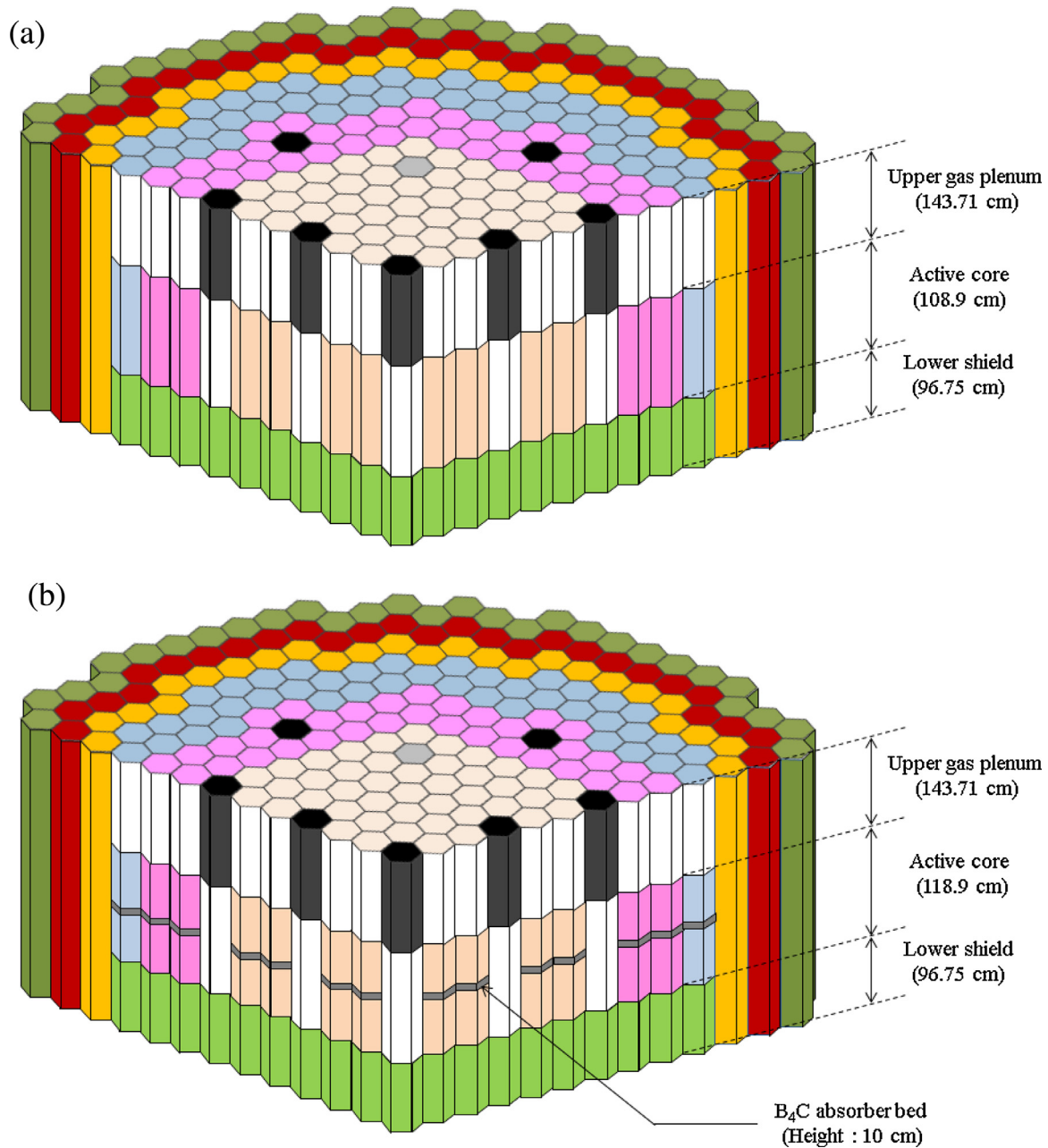


Fig. 3. 3-D configuration of the SFR 1/3 cores [(a) Proposed SFR type 1 core and typical SFR core, and (b) proposed SFR type 2 core.].

thermal-hydraulic design of a SFR has design constraints on the cladding temperature and the fuel temperature due to the high boiling temperature of the sodium coolant. Therefore, the maximum temperature which leads to damage of the cladding and fuel should be analyzed for the proposed SFR core design. The thermal-hydraulic design constraints of the SFR core are shown in Table 2.

The thermal-hydraulic design constraint pertaining to the fuel is the melting temperature. Due to the risk of fuel damage during a severe accident, the fuel temperature should be lower than

the melting temperature. For the proposed SFR core design, metal fuel is used. Its melting temperature is approximately 950 °C (Kim, 1994).

The constraint for the cladding is related to the cumulative damage fraction (CDF) limit. The cladding can be damaged by thermal creep, strain, swelling, and by other factors. The total damage by these factors is expressed as the CDF value, which is highly dependent on the cladding temperature. Under steady-state operation, the CDF limit is 0.001; this value corresponds to cladding temperatures of 625 °C for HT9 and 645 °C for the modified HT9 according to the work of Lee et al. (2009). The proposed SFR core design uses the modified HT9. Therefore, the cladding temperature should be lower than 645 °C.

To assess the core temperature distribution of a SFR core, KAERI developed the MATRA-LMR (Multichannel Analyzer for Transient and steady-state in Rod Array-Liquid Metal Reactor) code, a

Table 2
SFR core design constraints.

	Design constraint
Fuel centerline temperature (°C)	<950
Cladding temperature (°C)	<645

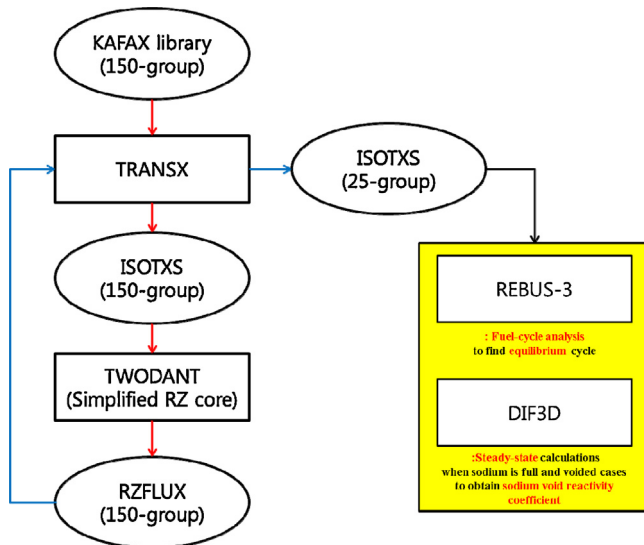


Fig. 4. Flow chart of the neutronics analysis code system for an SFR core.

sub-channel analysis code for liquid metal reactors. It is based on the MATRA code, which is a revision of the COBRA (COolant Boiling in Rod Arrays) code (Kim et al., 1999).

The major modifications and improvements implemented in the MATRA-LMR code are as follows:

1. Sodium property subprogram
2. Heat transfer coefficient correlation for sodium coolant
3. Most recent pressure drop correlations such as;
 - Novendstern correlation
 - Chiu–Rohsenow–Todreas correlation
 - Cheng–Todreas correlation

In the MATRA-LMR code, it is assumed that the sub-channel shape is triangular, as shown in Fig. 5. For each sub-channel, the MATRA-LMR code predicts the temperature, enthalpy and pressure according to the input data of the core geometric design and thermal-hydraulic conditions, such as the axial power distribution and the mass flow rate.

However, the MATRA-LMR code is not applicable to fuel assemblies containing moderating rods, which do not produce power. In MATRA-LMR, it is assumed that the radial heat flux distribution is uniform. To simulate the moderating rods, the source code of MATRA-LMR is modified in this study. In the modified MATRA-LMR code, a zero value is manually entered for the heat flux of the moderating rods. In this study, the existing and the modified MATRA-LMR codes are used for the thermal-hydraulic analyses of the typical fuel assembly and the modified fuel assembly, respectively.

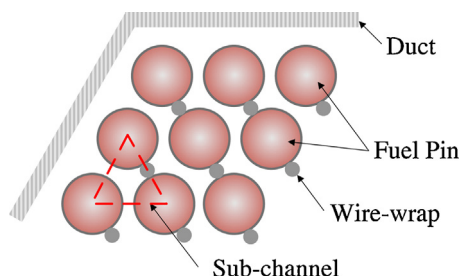


Fig. 5. Sub-channel in the fuel assembly.

Table 3

Core performance summary of the typical SFR.

Thermal power output	1500 MWth
Effective full power days	365 days
Number of fuel batch	5
Conversion ratio	1.02
Fuel material	U-TRU-10%Zr metallic alloy
Charged fuel TRU enrichment	15.03% TRU enrichment
Peak discharge fast neutron fluence	3.60E+23
Average discharged burnup	66.2 GWd/MTH
Radial assembly power peak (BOEC/EOEC)	1.25/1.25

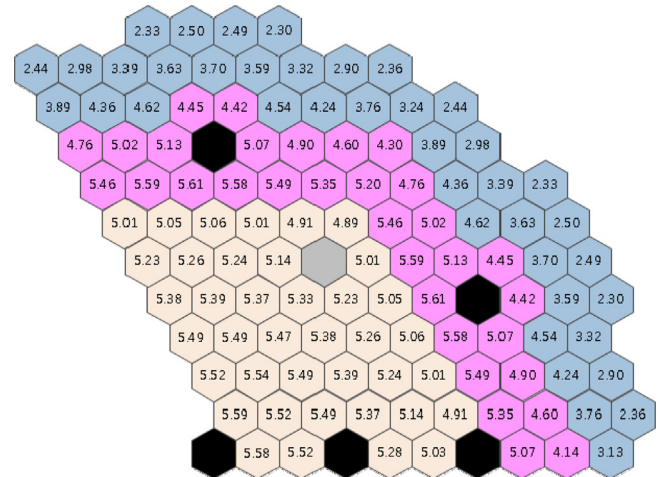


Fig. 6. Radial power distribution of the typical SFR design at EOEC (unit: MW).

4. Numerical results

4.1. Neutronics analysis results

Table 3 shows the performance summary of the typical SFR core, while Fig. 6 shows the radial power distribution of one third of the core at the end of an equilibrium cycle (EOEC).

There are five fuel batches to meet the peak discharge fast neutron fluence specification of $<4.0 \times 10^{23}$ neutrons/cm³. (For the proposed SFR design, a six-batch cycle is used.) At the end of an equilibrium cycle, the sodium void reactivity coefficients are calculated in various coolant void situations. The sodium void reactivity results are shown in Table 4.

As shown in Table 4, the sodium void reactivity coefficient is estimated to be 2397 pcm for the active-core-void situation. Most of this void reactivity comes from inner and mid-core voids (2269.325 pcm). For the outer core void situation, the reactivity insertion is about 100 pcm due to the increase in the neutron leakage caused by the coolant void. Fig. 7 shows the average neutron flux for each core region at the EOEC and the relative change in the neutron flux when the sodium at the active core region and its upper gas plenum region are voided.

Table 4

Sodium void reactivity coefficients in various void situations for a typical SFR.

Void case	Sodium void reactivity coefficient (pcm)
Active core void + upper gas plenum void	2397.773
Inner core void + upper gas plenum void	1465.434
Inner + mid core void + upper gas plenum void	2269.325
Mid + outer core void + upper gas plenum void	947.917
Outer core void + upper gas plenum void	101.406
Upper gas plenum void	−560.711

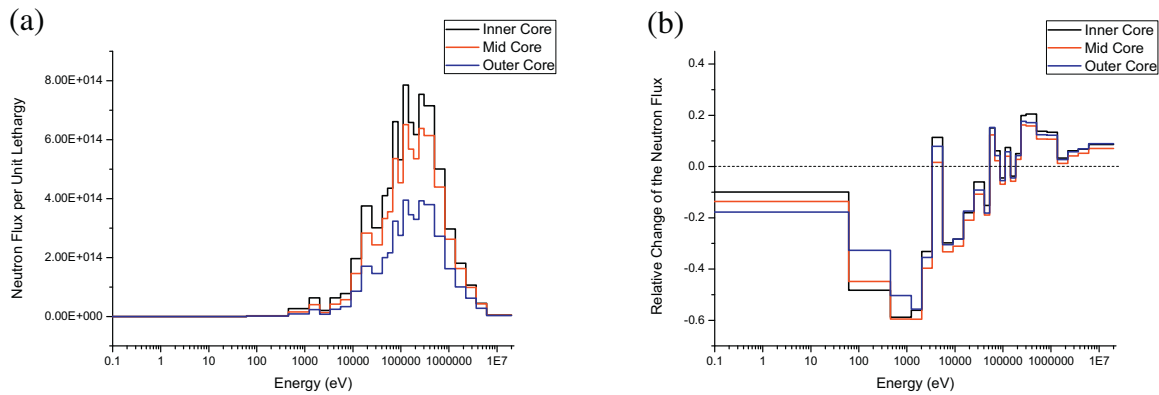


Fig. 7. (a) Average neutron flux for each core region at EOE (typical SFR core), and (b) relative change of the neutron flux when the sodium is voided.

Table 5

Core performance summary of the proposed SFR type 1.

Thermal power output	1500 MWth
Effective full power days	365 days
Number of fuel batch	6
Conversion ratio	0.97
Fuel material	U-TRU-10%Zr metallic alloy
Charged fuel TRU enrichment	18.66% TRU enrichment
Peak discharge fast neutron fluence	3.45E+23
Average discharged burnup	85.8 GWd/MTH
Radial assembly power peak (BOEC/EOEC)	1.23/1.29

Table 7

Core performance summary of the proposed SFR type 2.

Thermal power output	1500 MWth
Effective full power days	365 days
Number of fuel batch	6
Conversion ratio	0.73
Fuel material	U-TRU-10%Zr metallic alloy
Charged fuel TRU enrichment	29.6% TRU enrichment
Peak discharge fast neutron fluence	2.85E+23
Average discharged burnup	85.7 GWd/MTH
Radial assembly power peak (BOEC/EOEC)	1.37/1.32

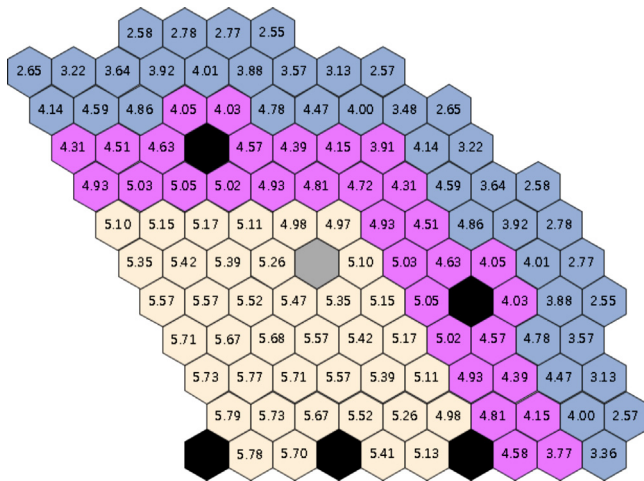


Fig. 8. Radial power distribution of the proposed SFR type 1 at EOE (unit: MW).

This typical SFR core result is used as a reference calculation for the proposed SFR design. First, the results for the proposed SFR type 1 core are shown in Table 5, Fig. 8, and Table 6.

The charged enrichment of TRU for the proposed SFR type 1 design is 18.66%. This value is greater than the reference design of

15.03%. The graphite-moderating rods are inserted into the inner and mid-region assemblies. Therefore, the total amount of the heavy metal inventory is decreased. To compensate for this for criticality, the charged fuel enrichment is increased.

As shown in Table 6, the sodium void reactivity coefficient for the active core void is greatly improved as compared to the reference design. Especially with regard to the case of an inner core void, it is reduced to nearly half that of the reference SFR design. This result shows that the graphite-moderating rod-replacement strategy for a SFR fuel assembly concept is feasible for enhancing the core safety with regard to the neutronics.

Fig. 9 shows the average neutron flux for each core region and the relative change of the neutron flux when sodium is voided for the proposed SFR type 1 core. Fig. 9(a) shows that the neutron flux is softened at the inner/mid-core regions compared to the typical SFR core results (Fig. 7(a)). Fig. 9(b) shows in a comparison with Fig. 7(b) that the neutron flux hardening effect at inner/mid-core regions when the coolant is voided is less than that of the typical SFR core. This occurs because the graphite rods act as a moderator even when the sodium is voided.

Next, Table 7, Fig. 10, and Table 8 show the neutronics analysis results of the proposed SFR type 2 core.

In this design, a B₄C absorber bed is inserted at the axial center of the active core. This B₄C absorber bed decouples the active core into upper and lower regions to increase the effective neutron

Table 6

Sodium void reactivity coefficients in various void situations for the proposed SFR type 1.

Void case	Sodium void reactivity coefficient (pcm)
Active core void + upper gas plenum void	1433.445
Inner core void + upper gas plenum void	772.810
Inner + mid core void + upper gas plenum void	1289.320
Mid + outer core void + upper gas plenum void	664.546
Outer core void + upper gas plenum void	118.434
Upper gas plenum void	−455.148

Table 8

Sodium void reactivity coefficients in various void situations for the proposed SFR type 2.

Void case	Sodium void reactivity coefficient (pcm)
Active core void + upper gas plenum void	1368.822
Inner core void + upper gas plenum void	541.639
Inner + mid core void + upper gas plenum void	1131.916
Mid + outer core void + upper gas plenum void	817.261
Outer core void + upper gas plenum void	192.312
Upper gas plenum void	−451.729

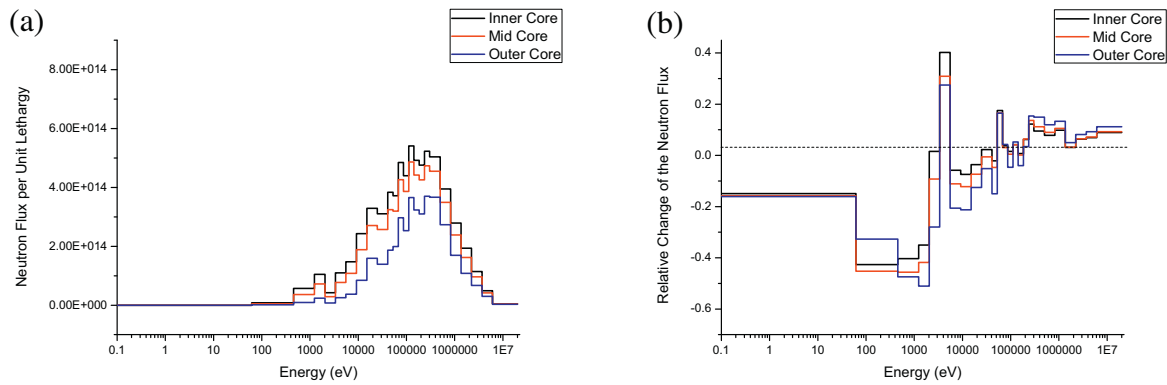


Fig. 9. (a) Average neutron flux for each core region at EOE (proposed SFR type 1 core), and (b) relative change of the neutron flux when the sodium is voided.

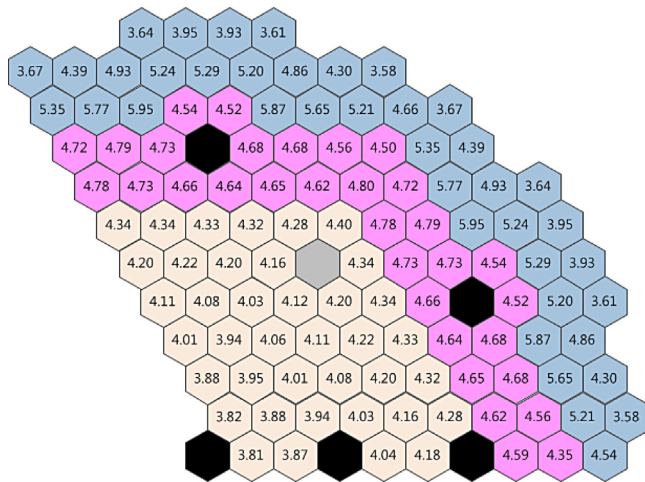


Fig. 10. Radial power distribution of the proposed SFR type 2 at EOE (unit: MW).

leakage. However, it degrades the neutron economy. The poor neutron economy increases the charged TRU enrichment to 29.6% (greater than the reference design of 15.03%). In addition, the conversion ratio is reduced to 0.73.

It was noted that the peak power fuel assembly is located in the outer core region, as shown in Fig. 10. In the type 2 SFR design, fuel rods are replaced by graphite-moderating rods in the inner and mid-region assemblies, as in the type 1 design. Therefore, the inner and mid-region assemblies have higher ratios of the B_4C absorber to the fuel content relative to those of the outer regions. As a result, the peak power fuel assembly moves from the inner core to the outer core.

The sodium void reactivity does not improve much compared to the proposed type 1 SFR design. The inner and mid-core void reactivity level is reduced by about 150 pcm; however, the outer core void reactivity is increased by approximately 74 pcm, as the fission reaction in the outer region is increased during normal operation.

Fig. 11 shows the average neutron flux for each core region and the relative change of the neutron flux when sodium is voided for the proposed SFR type 2 core. Fig. 11(a) shows that the neutron flux level is strongly decreased compared to the typical SFR core results. The B_4C absorber bed reduces the neutron economy, implying that a large increase in the charged TRU enrichment is necessary for core criticality, as discussed above. As shown in Fig. 11(b), neutron flux hardening at the inner core region when sodium is voided is not greatly reduced as compared to that in a typical SFR core. Therefore, the sodium void reactivity improvement is less than 70 pcm compared to that of the proposed SFR type 1 core, even if a B_4C absorber bed is introduced in the proposed SFR type 2 core design.

For the proposed SFR cores, the k_{eff} plot during the equilibrium cycle is shown in Fig. 12. For the proposed type 1 core, the multiplication factor is increased by about 250 pcm over the cycle. The conversion ratio for the type 1 reactor is 0.97, which is slightly less than unity. However, a large amount of U-238, a strong resonance absorber, is transmuted to the fissile material. This leads to an increase in the k_{eff} value. Otherwise, for the proposed SFR type 2 core, the conversion ratio is 0.73. Hence, the k_{eff} value is decreased by about 1400 pcm over the cycle.

4.2. Thermal-hydraulic analysis results

The methodology of a sub-channel analysis in the MATRA-LMR code is selected for the thermal-hydraulic analysis of the SFR core. Through the sub-channel analysis of the highest power assembly,

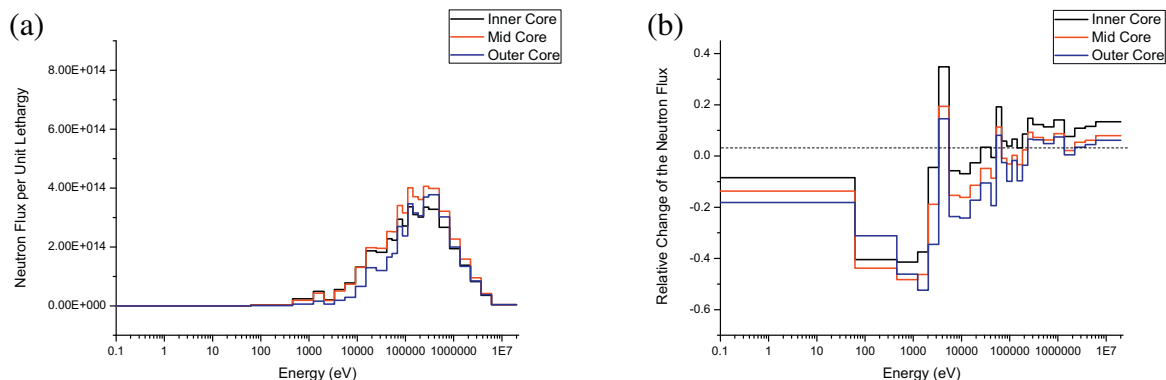


Fig. 11. (a) Average neutron flux for each core region at EOE (proposed SFR type 2 core), and (b) relative change of the neutron flux when the sodium is voided.

Table 9
Input parameters of the proposed SFR design for the MATRA-LMR code.

	Input parameters	Input value	
Geometric condition	Number of rod	271	
	Number of sub-channel	546	
	Rod diameter (mm)	9	
	Rod pitch (mm)	10.05	
	Wire diameter (mm)	1.4	
	Wire pitch (mm)	204.9	
	Total core length (mm)	3493.6 (Type 1, the typical SFR design)	3593.6 (Type 2)
Operating condition	Active core length (mm)	1089	
	Duct inside flat-to-flat distance (mm)	176.7	
	Pressure (MPa)	0.1013	
	Inlet temperature (°C)	390	

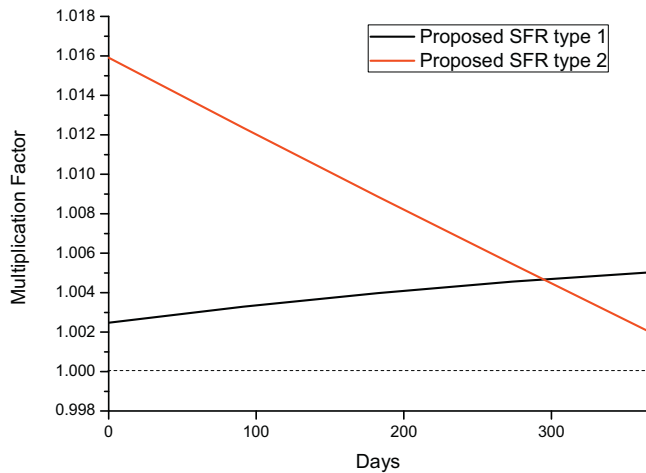


Fig. 12. k_{eff} change during the equilibrium cycle for the proposed SFR cores

the temperatures of the coolant, cladding and fuel are calculated and the mass flow rate is optimized to satisfy the design constraints. The main parameters for the geometric and operating conditions are listed in Table 9. The operating conditions are selected based on the KALIMER-600 design parameters.

In the typical SFR core, the hottest assembly is in the center of the core. For this assembly, the thermal-hydraulic analysis is conducted with the existing MATRA-LMR code. The axial temperature distributions of the coolant of the hottest sub-channel and the cladding and fuel of the hottest rod in the center of the assembly are shown in

Table 10
Optimized mass flow rate and maximum temperature in the typical SFR design.

Power of the hottest assembly at EOEC: 5.59 MW	
Optimized mass flow rate: 24.4 kg/s	
Maximum temperature (°C)	
Cladding	594.9
Fuel centerline	666.0

Fig. 13. In the core inlet (lower shield) at a height of 0–967.5 mm, the temperature values of the coolant, cladding and fuel are all identical because there is no heat flux in the lower shield region. In the core outlet (upper gas plenum) at a height of 2056.5–3496 mm, there are also no temperature differences among the coolant, cladding, and fuel. When the coolant flows upward at the active core region, the temperature of the coolant gradually increases and the temperature differences among the coolant, the cladding and the fuel cause heat flux. Therefore, the temperature peaks at the top of the active core region. The maximum temperature and optimized flow rate are shown in Table 10. The flow rate is optimized with a margin of 50 °C to the maximum allowable cladding temperature.

In the proposed SFR type 1, the hottest assembly is also in the center of the core. For this assembly, the sub-channel analysis was performed using the modified MATRA-LMR code. The 72 moderating rods have no power. In this assembly, the rod which has the highest temperature is in the corner. This results from the number of adjacent fuel rods. While most rods have three adjacent fuel rods, the rods in the three corners have five adjacent fuel rods. (The rods in the other three corners have two adjacent fuel rods.) The axial temperature distributions are shown in Fig. 14 and the main

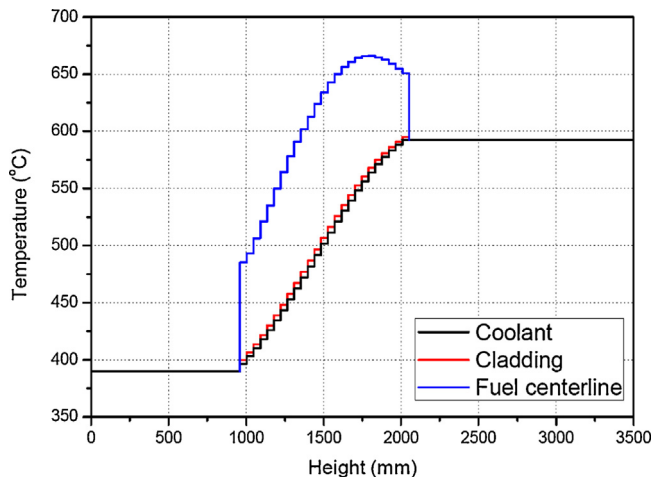


Fig. 13. Axial temperature distributions of the coolant, cladding and fuel for the hottest region in the typical SFR design.

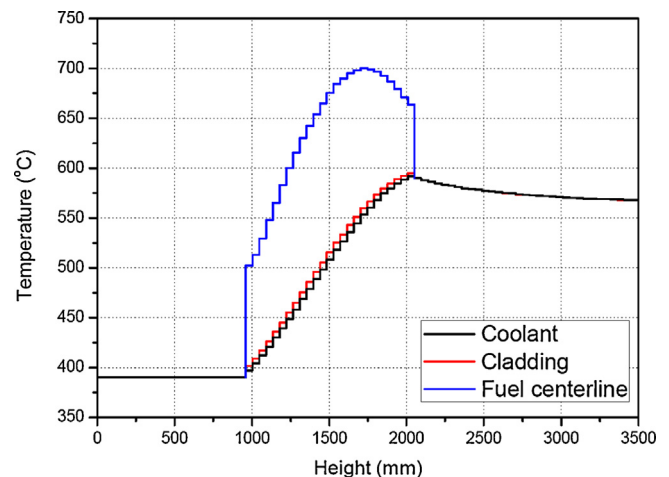


Fig. 14. Axial temperature distributions of the coolant, cladding and fuel for the hottest region in the proposed SFR type 1.

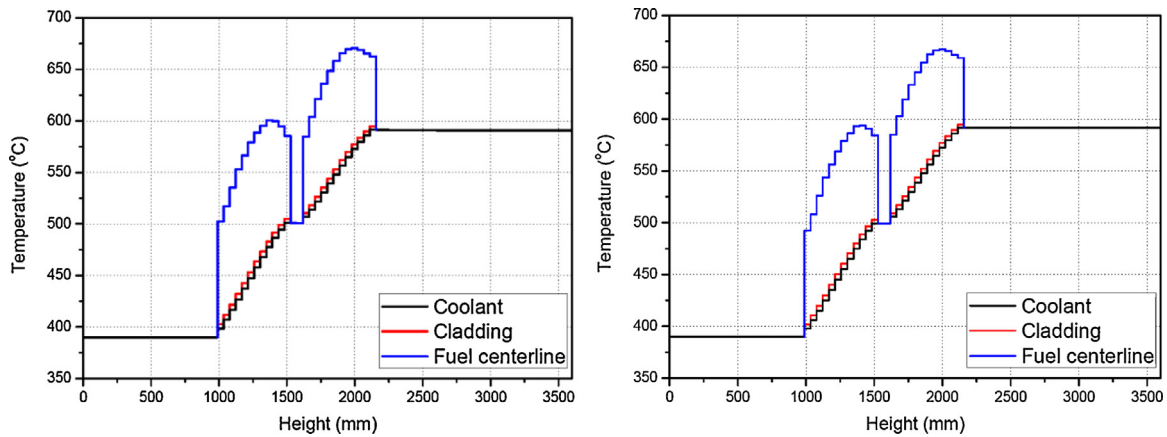


Fig. 15. Axial temperature distributions of the coolant, cladding and fuel for the hottest regions in the mid-core (left) and outer core (right) (proposed SFR type 2) regions.

Table 11

Optimized mass flow rate and maximum temperature in the proposed SFR type 1.

Power of the hottest assembly at EOEC: 5.79 MW	
Optimized mass flow rate: 26.3 kg/s	
Maximum temperature (°C)	
Cladding	594.9
Fuel centerline	700.4

results are listed in Table 11. As shown in Fig. 14, the temperature values are slightly decreased in the core outlet region (with a height of 2056.5–3496 mm). This temperature decrease results from the mixing with the coolant in the neighboring sub-channels near the duct wall. These outermost sub-channels have lower coolant temperatures than that in the sub-channel in the center of the assembly due to the relatively high mass flow rate. The mass flow rates are ~ 0.04 kg/s for the sub-channel in the center and 0.09 kg/s in the outermost sub-channel.

In the proposed SFR type 2, the outer core region contains the assembly which has the highest power in the core. However, the hottest assembly in the mid-core region contains the rod which has the highest power in the core. It is necessary to confirm which assembly is the hottest. For the assemblies in the mid-core region and the outer core region, the sub-channel analyses are conducted with the modified MATRA-LMR code and the existing MATRA-LMR code, respectively. As shown in Fig. 15, there are no temperature differences among the coolant, cladding and fuel in the middle of the fuel rod because the absorber sandwich region has no power output. The main results are summarized in Table 12. In the hottest assembly of the mid-core region, the optimized mass flow rate is lower than that in the hottest assembly of the outer core. This

indicates that the assembly in the outer core is the hottest throughout the core.

5. Summary and conclusions

A moderating rod-inserted SFR fuel assembly is proposed in this study to minimize the sodium void reactivity coefficient. By replacing some fuel rods with graphite-moderating rods, it is expected that neutron softening can be achieved even in a situation with coolant voids.

To determine the effect of moderating rods inserted into the SFR fuel assembly on the sodium void reactivity, two types of SFR cores were studied. The type 1 core adopts a new SFR fuel assembly design proposed in this study at the inner/mid-core regions. The type 2 core uses a B₄C absorber sandwich with a thickness of 10 cm at the center of the active core region as well as new SFR fuel assemblies at the inner/mid-core areas. Neutronics and thermal hydraulic analyses were performed on these two SFR core designs. In addition, a typical SFR core design based on the KALIMER-600 breakeven core was analyzed as a reference core.

In the neutronics analysis, the sodium void reactivity coefficient was determined in various void situations. In the case of sodium voiding in the active core and upper gas plenum, the two proposed core designs resulted in reductions of the sodium void reactivity coefficient of approximately 960–1030 pcm compared to the reference design. In the proposed SFR type 1, the TRU enrichment required is increased to 18.66% from the TRU enrichment 15.03% in the reference core. For the proposed SFR type 2, the TRU enrichment required is dramatically increased to 29.6% from the TRU enrichment 15.03% in the reference core. Despite the fact that a high TRU enrichment is required for the proposed SFR type 2 core, the sodium void reactivity coefficient reduction is less than 70 pcm as compared to that of the proposed SFR type 1 core.

In the thermal-hydraulic analysis, the temperature distribution is calculated for the typical SFR design and for the two proposed core designs with the existing and a modified version of the MATRA-LMR code. Through the sub-channel analysis, the mass flow rate was optimized to meet the design constraints for the highest power assembly. In the proposed SFR type 1, the hottest rod is in the corner of the assembly due to the number of adjacent fuel rods. In the proposed SFR type 2, it was found that the assembly in the outer region is the hottest throughout the core.

The results of this study indicate that the new SFR assembly design concept, which adopts graphite-moderating rods in the fuel assembly, is feasible for reducing the sodium void reactivity coefficient. The single TRU enrichment strategy and the single fuel slug diameter throughout the SFR core are also utilized because the

Table 12

Optimized mass flow rate and maximum temperature in the proposed SFR type 2.

Mid core	Power of the hottest assembly at EOEC: 4.80 MW	
	Optimized mass flow rate: 20.0 kg/s	
	Maximum temperature	
	Cladding	594.9 °C
Outer core	Power of the hottest assembly at EOEC: 5.95 MW	
	Optimized mass flow rate: 25.6 kg/s	
	Maximum temperature	
	Cladding	594.7 °C
	Fuel centerline	667.5 °C

radial power peak can be flattened according to the number of moderating rods in each core region. As a further study, detailed designs and analyses of other important reactivity coefficients and flow groupings are considered.

Acknowledgements

This work was supported in part by a grant from the National Research Foundation of Korea (NRF) funded by the Korean government (No. 2013-031155) and by the office of the KAIST EEWS Initiative (No. EEWS-2013-N01130019).

References

- Alcouffe, R.E., Baker, R.S., Brinkley, F.W., Marr, D.R., O'Dell, R.D., Walters, W.F., 1995. [DANTSYS: A Diffusion Accelerated Neutral Particle Transport Code System](#). LA-12969-M.
- Chang, Y.I., Hill, R.N., Fujita, E.K., Wade, D.C., Kumaoka, Y., Suzuki, M., Kawashima, M., Nakagawa, H., 1991. [Core concepts for "Zero-sodium-void-worth core" in metal fuelled fast reactor](#). In: Proc. International Conference on Fast Reactors and Related Fuel Cycles, Kyoto, Japan.
- Derstine, K.L., 1984. [DIF3D: A Code to Solve One-, Two-, and Three-Dimensional Finite-Difference Diffusion Theory Problems](#). ANL-82-64.
- Hahn, D., Kim, Y., Lee, C.B., Kim, S., Lee, J., Lee, Y., Kim, B., Jeong, H., 2007. [Conceptual design of the sodium-cooled fast reactor KALIMER-600](#). Nucl. Eng. Technol. 39, 193–206.
- Khalil, H.S., Hill, R.N., 1991. [Evaluation of liquid-metal reactor design options for reduction of sodium void worth](#). Nucl. Sci. Eng. 109, 221–226.
- Kim, Y.C., 1994. [Liquid Metal Reactor Development: Development of LMR Design Technology](#). KAERI/RR-1396/93.
- Kim, W.S., Kim, Y.G., Kim, Y.J., 1999. [A User's Guide to the MATRA-LMR Code](#). KAERI/TR-1291/99.
- Lee, B.O., Cheon, J.S., Ryu, H.J., Kim, J.H., Yang, S.W., Lee, C.B., 2009. [Performance evaluation of metallic fuel for SFR](#). In: Proc. International Congress on Fast Reactors and Related Fuel Cycles: Challenges and Opportunities, Kyoto, Japan.
- MacFarlane, R.E., 1992. [TRANSX2: A Code for Interfacing MATXS Cross-Section Libraries to Nuclear Transport Codes](#). LA-12312-MS.
- MacFarlane, R.E., Muir, D.W., 1994. [The NJOY Nuclear Data Processing System Version 91](#). LA-12740-M.
- Rachi, M., Yamamoto, T., Jena, A.K., Takeda, T., 1997. [Parametric study on fast reactors with low sodium void reactivity by the use of zirconium hydride layer in internal blanket](#). J. Nucl. Sci. Technol. 34, 193–201.
- Toppel, B.J., 1990. [A User's Guide for the REBUS-3 Fuel Cycle Analysis Capability](#). ANL-83-2.